Using Time-Reversal Symmetry for Sensitive Incoherent Matter-Wave Sagnac Interferometry

Y. Japha, O. Arzouan, Y. Avishai, and R. Folman
Department of Physics, Ben-Gurion University, Be'er-Sheva 84105, Israel
(Received 6 December 2006; published 8 August 2007)

We present a theory of the transmission of guided matter-waves through Sagnac interferometers. Interferometer configurations with only one input and one output port have a property similar to the phase rigidity observed in the transmission through Aharonov-Bohm interferometers in coherent mesoscopic electronics. This property enables their operation with incoherent matter-wave sources. High rotation sensitivity is predicted for high finesse configurations.

DOI: 10.1103/PhysRevLett.99.060402 PACS numbers: 03.75.Be, 07.60.Ly, 73.63.−b

The Sagnac effect in a wave propagating through a closed rotating ring induces a phase shift proportional to the angular frequency Ω of this rotation and the area A of the ring [1]. For light waves with frequency ω this phase shift is $\phi_{\text{light}} = (2\omega A/c^2)\Omega$, where c is the speed of light. For de Broglie waves of nonrelativistic particles with mass m, the phase shift is $\phi_{\text{matter}} = (2mA/\hbar)\Omega = (mc^2/\hbar\omega)\phi_{\text{light}}$ [2,3], so that the rotation sensitivity of a matter-wave Sagnac interferometer (SI) is potentially better by a factor of $\sim 10^{11}$. First experimental attempts demonstrated rotation sensitivities comparable to or even better than those of the optical SI [4–6]. However, these "one-pass" SIs are limited by their small effective area and the relatively low flux available from coherent matter-wave sources. Light SIs with "multipass" configurations ("high finesse"), such as ring laser gyros, use larger effective area to improve rotation sensitivity. Recently dynamic magnetic potentials [7] and waveguide ring structures for cold atoms [8,9] were demonstrated, opening the door for the development of multipass guided atomic Sagnac interferometry.

In this Letter we use the analogy [10] between the Sagnac effect for massive neutral particles and the Aharonov-Bohm (AB) effect in coherent electron transmission through mesoscopic rings [11]. AB interferometers with only two ports connected to the ring show "phase rigidity" of the transmission pattern as a function of the magnetic flux Φ, when an effective path length difference between the interferometer arms is introduced [12,13]. Because of time-reversal invariance and current conservation in any system with two ports, the transmission is invariant under magnetic field inversion $\Phi \rightarrow -\Phi$. This property, when applied to atom SIs, leads to their robustness under effective path length differences and enables their operation with high-finesse and incoherent sources, which are available with higher particle flux. SIs of this kind may increase rotation sensitivity or may enable miniaturization onto atom chips [14] without suppressing it.

In general, a SI consists of a loop and one or more junctions, each consisting of one or more beam splitters (BS) connecting the loop to input and output channels. Here we consider a 1D model where each waveguide permits a single transverse mode, but finally show how to extend it to the multimode case. In 1D, a linear junction with n_p ports is represented by a $n_p \times n_p$ unitary scattering matrix S connecting the output amplitudes to the input amplitudes at the ports. As demonstrated in Fig. 1 we denote the indices of the ports of the input junction connected to the SI loop by α and β with corresponding input and output amplitudes $a_\pm$ and $b_\pm$, while the input amplitude a_{in} (normalized to $a_{\text{in}} = 1$) is incident from port i. The amplitudes are then related by

$$\begin{pmatrix} a_+ \\ b_+ \end{pmatrix} = \begin{pmatrix} S_{\alpha i} \\ S_{\beta i} \end{pmatrix} a_{\text{in}} + \begin{pmatrix} S_{\alpha\alpha} & S_{\alpha\beta} \\ S_{\beta\alpha} & S_{\beta\beta} \end{pmatrix} \begin{pmatrix} a_- \\ b_- \end{pmatrix}. \quad (1)$$

If the system is linear, then the amplitudes a_-, b_- are related to the amplitudes a_+, b_+ by

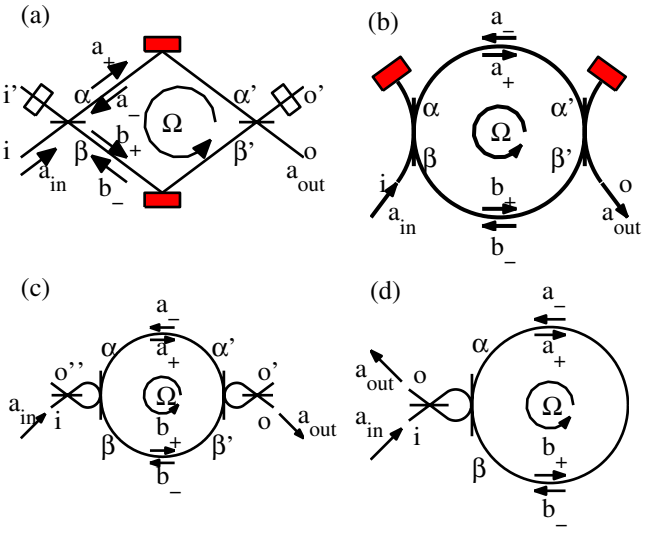

FIG. 1 (color online). Geometries of guided matter-wave Sagnac interferometers: (a) MZ. Open squares mean controllable reflectivity. When fully (not) reflecting we name the interferometer: closed (open) MZ. (b) 2-port loop. Closed squares are fully reflecting mirrors. (c) 4-port loop. (d) Single junction loop. In all configurations horizontal lines mean 50%–50% BSs while vertical lines mean BSs with a transmission amplitude it.

$$\begin{pmatrix} a_- \\ b_- \end{pmatrix} = S_L \begin{pmatrix} a_+ \\ b_+ \end{pmatrix}, \tag{2}$$

where a_- and b_- are taken at the internal ports α and β and the 2×2 S matrix $S_L(k, \Omega)$ describes the transmission through the loop, thereby containing terms of the form $e^{i(kL \pm \phi)}$, $\hbar k$ being the longitudinal momentum of the particles, L the circumference of the loop and ϕ the rotational phase shift. S_L is in general nonunitary when particles can leave the loop from another junction, such as through port o in Fig. 1(a). Time-reversal symmetry (Onsager relations [15]) implies that $S_{\alpha\beta} = S_{\beta\alpha}$ and that S_L has the form

$$S_L = \begin{pmatrix} a & be^{i\phi} \\ be^{-i\phi} & c \end{pmatrix},$$

where a, b, and c are functions of k. By substituting Eq. (2) into Eq. (1) we obtain an equation that can be solved either directly or as a perturbation expansion

$$\begin{pmatrix} a_+ \\ b_+ \end{pmatrix} = \frac{1}{I - T} \begin{pmatrix} S_{\alpha i} \\ S_{\beta i} \end{pmatrix} a_{\text{in}} = \sum_{n=0}^{\infty} T^n \begin{pmatrix} S_{\alpha i} \\ S_{\beta i} \end{pmatrix}, \tag{3}$$

where I is the 2×2 unity matrix and $T = \tilde{S} S_L$, $\tilde{S}$ being the submatrix of S appearing in Eq. (1). The matrix T is proportional to e^{ikL} and has eigenvalues whose modulus is always smaller than 1. This permits the perturbation expansion in T, where a_+, b_+ are described as a sum of partial waves $a_+ = \sum_{n=0}^{\infty} a_+^{(n)}$, $b_+ = \sum_{n=0}^{\infty} b_+^{(n)}$ such that T relates the nth terms, describing waves propagating a distance of nL along the loop, to the $(n-1)$th term. The output of the SI is obtained when propagating the amplitudes a_+, b_+ through the SI arms and transmitting them into the output port through the output junction. If no imperfections exist in the arms, the output amplitude at port o is given by

$$a_{\text{out}} = S'_{o\alpha'} e^{i(k - \phi/L)L_\alpha} a_+ + S'_{o\beta'} e^{i(k + \phi/L)L_\beta} b_+, \tag{4}$$

where S' is the scattering matrix of the output junction and L_α, L_β are the lengths of the corresponding arms, such that $L = L_\alpha + L_\beta$.

Time-reversal symmetry, which determines the symmetry properties of the scattering matrices $\tilde{S}$ and S_L discussed above yields the following form of the transmission through the SI, true for any geometry [13]

$$P(k, \phi) = |a_{\text{out}}|^2 = \frac{B + C\cos(\phi + \gamma)}{1 + D\cos\phi + H\cos^2\phi}, \tag{5}$$

where B, C, D, H, and γ are functions of k. When the SI has only one input and one output port, time-reversal symmetry and current conservation imply that $P(\phi) = P(-\phi)$, so that $\gamma = 0$ or $\gamma = \pi$ (phase rigidity). In what follows we show that while in an SI having more than two open ports γ may be strongly k dependent, such that an integration over a wide momentum bandwidth Δk washes out the ϕ dependence of $P(\phi)$, this dependence is conserved in an SI having only 2 open ports and fixed γ, enabling wide bandwidth operation.

Let us first examine a simple SI which does not satisfy the condition for phase rigidity. The Mach-Zehnder (MZ) SI shown in Fig. 1(a) is analogous to the SI implemented in [6]. It contains two 50%–50% junctions where an incident particle may be either reflected with amplitude $S_{\beta,i} = S_{\alpha,i'} = 1/\sqrt{2}$ or transmitted with amplitude $S_{\alpha,i} = S_{\beta,i'} = i/\sqrt{2}$. This is a one-pass SI with no reflections from the loop ports α and β back into the loop ($\tilde{S} = S_L = T = 0$), so that the transmission probability at the output port o is $P(k, \phi) = \sin^2[(\phi - k\delta L)/2]$, where $\delta L = L_\alpha - L_\beta$ is the length difference between the SI arms. $P(k, \phi)$ has the form (5) with $B = -C = 1/2$, $D = H = 0$ and $\gamma = k\delta L$. If $\delta L \neq 0$ and the input flux has a Gaussian spectrum $G(k)$ of bandwidth Δk around $k = \bar{k}$, then the time-averaged transmission probability $P(\Omega) = \int dk G(k) P(k, \phi(\Omega))$ becomes

$$P(\Omega) = \frac{1}{2}\left[1 - \eta \cos\left(\frac{2mA}{\hbar}\Omega - \bar{k}\delta L\right)\right], \tag{6}$$

where the interference visibility $\eta = e^{-\Delta k^2 \delta L^2/2}$ decreases with momentum bandwidth and path difference. If, in addition, the atomic beam is not perfectly collimated so that parts of it take paths surrounding different effective area with uncertainty δA, then η is multiplied by a factor $\exp[-(2m/\hbar)^2 \delta A^2 \Omega^2/2] = \exp[-(\delta A^2/A^2)\phi^2/2]$. Both suppression factors have been observed experimentally, as demonstrated in Fig. 3 of Ref. [6].

In contrast, we now study a closed loop SI obtained by closing the ports i' and o' of the MZ with mirrors placed in front of them [Fig. 1(a)], so that each junction now has only 3 open ports. A particle incident from one of the loop arms on such a junction may be reflected back into one of the loop arms with amplitudes given by

$$\tilde{S} = \frac{e^{i\theta}}{2}\begin{pmatrix} 1 & i \\ i & -1 \end{pmatrix}, \quad S_L = \frac{e^{i(kL + \theta')}}{2}\begin{pmatrix} e^{ik\delta L} & ie^{i\phi} \\ ie^{-i\phi} & -e^{-ik\delta L} \end{pmatrix}, \tag{7}$$

where θ, θ' are phases due to reflection at the mirrors. Following the above prescription, we obtain the transmission probability as in (5) with $\gamma = 0$, such that $P(\phi) = P(-\phi)$. In view of Eqs. (3) and (4), it is now insightful to note that the output amplitude can be written as a sum $a_{\text{out}} = \sum_{n=0}^{\infty} a_n e^{i(n+1/2)kL}$, where the amplitudes a_n contain the terms $e^{\pm ik\delta L}$, which are slowly oscillating relative to the fast oscillation of e^{inkL}, if $\delta L \ll L$. In the transmission probability $P(k, \phi) = |a_{\text{out}}|^2$ fast oscillations appear in cross terms $a_n^* a_{n'}$, with $n \neq n'$ describing interference between trajectories with different number of passes through the loop in either direction. In a realistic situation where the coherence length of the matter-wave source is much smaller than L ($\Delta k \gg 2\pi/L$), these interference terms will be eliminated. We may then define a slowly varying time-averaged transmission probability integrated over a period $2\pi/L$ of the fast oscillations

$$\bar{P}(k,\phi) \equiv \left(\frac{L}{2\pi}\right)\int_{k-\pi/L}^{k+\pi/L} dk' |a_{\rm out}(k',\phi)|^2 \approx \sum_{n=0}^{\infty} |a_n|^2, \quad (8)$$

describing the transmission of a quasimonochromatic flow ($\Delta k \delta L \ll 1$), where the coherence length is large relative to effective path length differences between trajectories with the same number of passes. In the incoherent limit where $\Delta k \delta L \gg 1$, integration of $P(k,\phi)$ over the bandwidth is equivalent to taking the average of $\bar{P}$ over $0 < k\delta L < 2\pi$. In this limit only paths with exactly the same length may interfere.

The closed MZ transmission probability in the quasimonochromatic case is found to be

$$\bar{P} = \frac{1 - \frac{1}{2}(\cos^2 k\delta L + \cos^2\phi)}{1 - \frac{1}{4}(\cos k\delta L - \cos\phi)^2}, \quad (9)$$

as shown in Fig. 2(a) for a few values of $k\delta L$ (thin curves). In the incoherent limit (thick curve) the visibility is not suppressed as in the open MZ but stays fixed at $\eta = 0.1813$. This residual visibility may be understood as interference between counterpropagating waves that follow trajectories with exactly equal lengths, as in white light interferometry. The relative phase between these waves depends only on the rotation frequency Ω but not on k. In the closed MZ the existence of such pairs of interfering trajectories is allowed by internal reflections, which in a system with a single transverse mode are an inevitable result of current conservation in a junction with only three ports (as in the AB experiments).

The rotation sensitivity is the minimal rotation frequency change $\delta\Omega_{\rm min}$ that generates a noticeable SI transmission change (beyond noise level). For an average incident flux F with a Poissonian particle number distribution, it is

$$\delta\Omega_{\rm min} = \frac{\hbar}{2mA}\frac{\delta\phi_{\rm min}}{\sqrt{F\tau}}, \quad \delta\phi_{\rm min} = \sqrt{P(\phi)}\left|\frac{\partial P}{\partial\phi}\right|^{-1}, \quad (10)$$

where τ is the measurement time and $\delta\phi_{\rm min}$ the dimensionless phase sensitivity per particle. The best sensitivity is achieved near points with maximal derivative $P'(\phi)$. For SIs with sinusoidal transmission as the open or closed MZ, the best sensitivity is inversely proportional to the visibility. In particular for the incoherent closed MZ $\delta\phi_{\rm min} = \sqrt{1+\eta}/2\eta \approx 3$ at $\phi = \pi/4$.

In order to achieve better rotation sensitivity we now turn our attention to SIs with a high-finesse loop. The finesse $\mathcal{F} = (2\pi/L)/\Delta_k$ is inversely proportional to the resonance bandwidth $\Delta_k = (1-R)/\sqrt{R}L$, R being the probability to stay in the loop for a full round trip. For a high-finesse loop ($R \approx 1$), $\mathcal{F}$ is proportional to the average number of passes of a particle through the loop before exiting through a junction. The closed MZ SI can be converted into a high-finesse SI by replacing its BS with a "vertical" BS rotated by 90° relative to the MZ BS [Fig. 1(b)]. A particle incident on the vertical BS has reflection and transmission amplitudes r and $it = i\sqrt{1-r^2}$, which are controllable, for example, with a magnetic tunneling barrier as suggested in [16]. $\mathcal{F} \gg 1$ requires that $r \approx 1$ and $t \ll 1$. Here the transmission amplitude between the two arms $S_{\alpha\beta} = S_{\beta\alpha} = r$, while back reflection through the mirror is only permitted to arm $\beta\beta'$ with amplitude $S_{\beta\beta} = -t^2 e^{i\theta}$. An analysis similar to that of the closed MZ yields the quasimonochromatic transmission probability shown in Fig. 2(b) for different values of $k\delta L$ (thin curves). The transmission has a symmetric dip at $\phi = 0$, whose depth and width depend on the value of $k\delta L$. Its width for a given value of $k\delta L$ is proportional to $\Delta_k = (1-r^4)/r^2 L \approx 2t^2/rL$ and inversely proportional to $\mathcal{F} \approx \pi r/t^2$. In the incoherent limit (thick curve), $\bar{P}(\phi) \approx P_0[1 - \mu\mathcal{L}(\phi)]$, where $P_0 \approx t^2/r$, $\mathcal{L}(\phi)$ is a Lorentzian of FWHM $\Delta_\phi \sim \Delta_k L$ and $\mu \approx 0.2935$ [visibility $\eta = \mu/(2-\mu) \approx 0.172$]. Using Eq. (10), the best sensitivity near $\phi \approx \pm\Delta_\phi/2$ is $\delta\phi_{\rm min} \sim \Delta_\phi/\sqrt{P_0}/\eta \approx \sqrt{2\Delta_\phi}/\eta_\phi \propto \mathcal{F}^{-1/2}$. The transmission dip is due to destructive interference between pairs of equal length paths

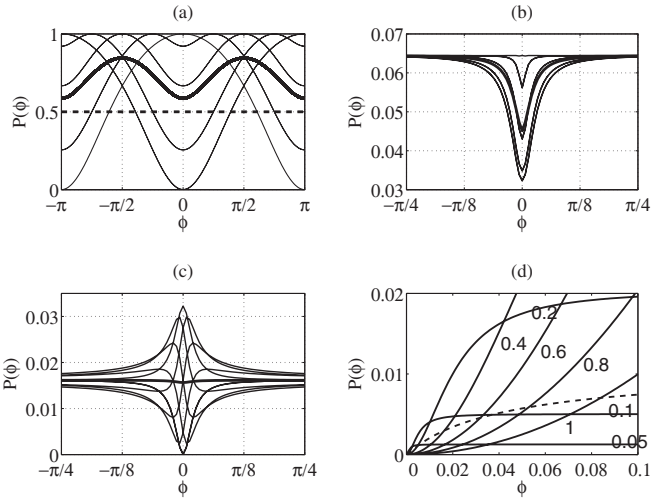

FIG. 2. Transmissivity of Sagnac interferometers as a function of rotational phase shift ϕ (a) closed MZ. (b) 2-port loop. (c) 4-port loop. (d) single junction loop. Thin curves in plots (a)–(c) represent the quasimonochromatic transmission $\bar{P}(\phi)$ for few values of phase difference between the two arms $k\delta L$ and thick curves represent the transmission in the incoherent limit. The dashed curve in (a) represents the open MZ transmission in the incoherent limit. In (b)–(c) the BS transmission amplitude is $t = 0.25$. Comparison of the closed and open MZ in (a), and comparison of (b) and (c), demonstrate how time-reversal symmetry $\bar{P}(\phi) = \bar{P}(-\phi)$ preserves the visibility when averaged over $k\delta L$ (incoherent limit). In (d) solid curves represent transmission $\bar{P}(\phi)$ for few values of t (numbers) and the dashed curve is the transmission for an incident thermal mixture of 101 transverse modes j with $0 < t_j < 1$ (equal spacing) and $n_j^{(\rm in)} \propto e^{-\kappa t_j}$ ($\kappa = 10$). Transmission at small ϕ is dominated by low t_j states (high finesse). The dip in the incoherent signal of (b) and (d) at $\phi = 0$ is due to destructive interference between exact same length trajectories (due to $\pi/2$ phase difference between the r and t amplitudes).

when $\phi = 0$. For comparison, we calculated the transmission of a similar high-finesse SI with additional ports using a combination of a 50%–50% BS and a vertical BS at each junction [Fig. 1(c)]. The quasimonochromatic transmission of this SI [thin curves in Fig. 2(c)] is not symmetric about $\phi = 0$ and the visibility drops to 0 in the incoherent limit (thick curve).

Finally, we utilize the formalism developed here to analyze a simple SI where each trajectory has a counterpropagating counterpart of the same length. The SI configuration in Fig. 1(d) contains only one junction for input and output. Its output amplitude is obtained by substituting $L_\alpha = L_\beta = L$ and $S' = S$ in Eq. (4). The matrix T for this SI is diagonal, corresponding to no coupling between counterpropagating modes, but on the other hand, all trajectories of the same order n have exactly the same length, giving rise to destructive interference at $\phi = 0$. The slowly varying transmission probability (8) is then a sum over k independent contributions $t^4 r^{2n} \sin^2[(n+1)\phi]$ resulting in the following transmission, which holds both for quasimonochromatic and incoherent inputs

$$\bar{P}(\phi) = \frac{t^2}{1+r^2}\left[1 - \frac{\cos^2\phi}{1 + 4(r/t^2)^2 \sin^2\phi}\right] \qquad (11)$$

with a Lorentzian dip at $\phi = 0$ of FWHM $\Delta_\phi = t^2/r$, full visibility ($\eta = 1$) and an asymptotic transmission $P_0 \approx t^2/2r$, as shown in Fig. 2(d) (solid curves) for different values of t. The best sensitivity at $\phi \to 0$ is $\delta\phi_{\min} \approx t/(2\sqrt{2r}) = \sqrt{\Delta_\phi/8}$, which scales as $\mathcal{F}^{-1/2}$, with $\mathcal{F} = 2\pi r/t^2$.

To extend the single mode model to the multimode case where the waveguide supports $N > 1$ transverse modes, we replace the amplitudes a_{in}, a_{out}, $a_\pm$ and $b_\pm$ with N component vectors and the matrices $\tilde{S}$, S_L and T with $2N \times 2N$ matrices. If different transverse modes j have different tunneling amplitudes t_j, then in the absence of mode mixing the transmission of an incident thermal flux with $n_j^{(\text{in})}$ particles in mode j is the sum $N_{\text{out}}(\phi) = \sum_j n_j^{(\text{in})} \bar{P}_j(\phi)$. For the single junction SI [Eq. (11)] one always finds $\bar{P}_j(\phi = 0) = 0$ and at small ϕ the transmission is dominated by the modes with low t_j (high finesse), as seen in Fig. 2(d), where we demonstrate the transmission for a multimode input with $n_j^{(\text{in})} \propto e^{-\kappa t_j}$ (dashed curve). In the presence of symmetric mode mixing and phase dispersion, $\bar{P}(\phi)$ still vanishes at $\phi = 0$ and our numerical analysis shows that the transmission is not significantly affected, due to the strong symmetry of the device.

To estimate the sensitivity of a Sagnac atom chip, we assume a waveguide ring of radius 1 cm about 10 μm above the chip surface with magnetic field gradients of the order $|\nabla \mathbf{B}| \sim 1$ G/μm. The centrifugal force mv^2/r of the circulating atoms must not exceed $\mu_B |\nabla \mathbf{B}|$. This limits the maximum velocity of the atoms to $v \sim 10$ m/sec. An atomic trap lifetime of about 10 s permits up to 1000–2000 rotations, corresponding to a tunneling amplitude $t \sim 0.035$ at the BS. For the single junction loop we obtain $\delta\phi_{\min} \sim 0.013$. If we assume that 1% of the available flux of above 10^9 s^{-1} (e.g., 2D MOT [17]) can be loaded into the waveguide, we obtain a sensitivity of $\delta\Omega < 5 \times 10^{-12}$ rad s$^{-1}/\sqrt{\text{Hz}}$, ~2 orders of magnitude better than the best value published to date [18].

The above theoretical model will enable a more comprehensive study of multimode operation and the effect of dispersion and imperfections in the SI components, which is needed before applying the suggestions in this Letter to real systems. Other effects such as Berry phase in a magnetic ring potential [19] and atom-atom collisions in a system of bosons or fermions should be studied as well.

We thank Daniel Rohrlich, Ora Entin-Wohlman, and Amnon Aharony for useful discussions. R. F. thanks Yoseph Imry for discussions on quantum interferometry. We acknowledge the support of the EC "atomchip" (RTN) consortium, the German Federal Ministry of Education and Research (BMBF-DIP project), the American-Israeli Foundation (BSF), and the Israeli Science Foundation.

[1] For a recent review, see I. A. Andronova and G. B. Malykin, Phys. Usp. **45**, 793 (2002).
[2] F. Hasselbach and M. Nicklaus Phys. Rev. A **48**, 143 (1993).
[3] S. A. Werner, J.-L. Staudenmann, and R. Colella, Phys. Rev. Lett. **42**, 1103 (1979).
[4] F. Riehle *et al.*, Phys. Rev. Lett. **67**, 177 (1991).
[5] A. Lenef *et al.*, Phys. Rev. Lett. **78**, 760 (1997).
[6] T. L. Gustavson, P. Bouyer, and M. A. Kasevich, Phys. Rev. Lett. **78**, 2046 (1997).
[7] G.-B. Jo *et al.*, Phys. Rev. Lett. **98**, 030407 (2007).
[8] A. S. Arnold, C. S. Garvie, and E. Riis, Phys. Rev. A **73**, 041606 (2006).
[9] I. Lesanovsky *et al.*, Phys. Rev. A **73**, 033619 (2006).
[10] J. J. Sakurai, Phys. Rev. D **21**, 2993 (1980).
[11] Y. Imry, *Introduction to Mesoscopic Physics* (Oxford University, New York, 1997).
[12] M. Büttiker, Phys. Rev. Lett. **57**, 1761 (1986); A. Levy Yeyati and M. Büttiker, Phys. Rev. B **52**, R14 360 (1995).
[13] A. Aharony, O. Entin-Wohlman, B. I. Halperin, and Y. Imry, Phys. Rev. B **66**, 115311 (2002).
[14] R. Folman *et al.*, Adv. At. Mol. Opt. Phys. **48**, 263 (2002); J. Reichel, Appl. Phys. B **74**, 469 (2002).
[15] L. Onsager, Phys. Rev. **38**, 2265 (1931); H. B. G. Casimir, Rev. Mod. Phys. **17**, 343 (1945);
[16] E. Andersson, M. T. Fontenelle, and S. Stenholm, Phys. Rev. A **59**, 3841 (1999); J. A. Stickney and A. A. Zozulya, Phys. Rev. A **68**, 013611 (2003).
[17] R. S. Conroy *et al.*, Opt. Commun. **226**, 259 (2003); Y. B. Ovchinnikov, Opt. Commun. **249**, 473 (2005).
[18] T. L. Gustavson, A. Landragin, and M. A. Kasevich, Classical Quantum Gravity **17**, 2385 (2000).
[19] P. Zhang and L. You, Phys. Rev. A **74**, 062110 (2006).